Article

Mechanistic Studies on the Cyclization of (*Z*)-1,2,4-Heptatrien-6-yne in Methanol: A Possible Nonadiabatic Thermal Reaction

Matthew E. Cremeens, Thomas S. Hughes, and Barry K. Carpenter

J. Am. Chem. Soc., **2005**, 127 (18), 6652-6661• DOI: 10.1021/ja0445443 • Publication Date (Web): 14 April 2005

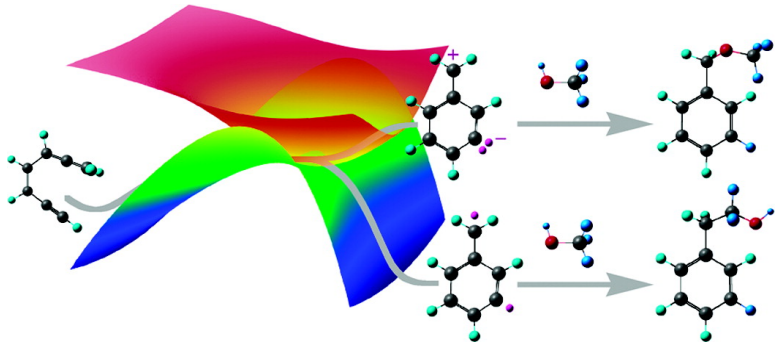

More About This Article

Additional resources and features associated with this article are available within the HTML version:

- Supporting Information
- Links to the 1 articles that cite this article, as of the time of this article download
- Access to high resolution figures
- Links to articles and content related to this article
- Copyright permission to reproduce figures and/or text from this article

View the Full Text HTML

J|A|C|S
ARTICLES
Published on Web 04/14/2005

Mechanistic Studies on the Cyclization of (*Z*)-1,2,4-Heptatrien-6-yne in Methanol: A Possible Nonadiabatic Thermal Reaction

Matthew E. Cremeens,[†] Thomas S. Hughes,[‡] and Barry K. Carpenter*

Contribution from the Department of Chemistry and Chemical Biology, Baker Laboratory, Cornell University, Ithaca, New York 14853-1301

Received September 9, 2004; E-mail: bkc1@cornell.edu

Abstract: Myers et al. pyrolyzed (*Z*)-1,2,4-heptatrien-6-yne (**1**) in methanol at 100 °C and observed benzylmethyl ether (**2**) as a major product and 2-phenylethanol (**3**) as a minor product. If a biradical intermediate, such as the open-shell singlet state of α,3-didehydrotoluene (**4**), was the only intermediate generated by the cyclization, then reaction with methanol might be expected to afford 2-phenylethanol as the principal product. The question that has been of interest since its first discovery is the origin of the principal product of the title reaction, benzylmethyl ether. This report considers three mechanisms for formation of the benzylmethyl ether: direct methanol participation in the cyclization of the reactant, partial ether formation from the biradical **4**, or involvement of the closed-shell zwitterionic state of α,3-didehydrotoluene (**5**). A fourth mechanism, involving a cyclic allene intermediate, has been ruled out by earlier studies. In the present work, the first two mechanisms are ruled out by experiment and/or calculation. The remaining one, involving the zwitterion, is shown to be consistent with experimental and computational data only if a component of the reaction follows a nonadiabatic course.

Introduction

The proposed mechanism of action of the antitumor antibiotic neocarzinostatin involves the cyclization of an enyne cumulene to generate a reactive biradical intermediate (Figure 1).[1,2] Interest in this crucial step led to the synthesis and pyrolysis of the least substituted version of this enynecumulene core, (*Z*)-1,2,4-heptatrien-6-yne or enyneallene.[3]

The Mechanistic Question. Myers et al. pyrolyzed enyneallene (**1**) in methanol at 100 °C and observed benzylmethyl ether (**2**) as a major product and 2-phenylethanol (**3**) as a minor product (Figure 2).[3] If a biradical intermediate, such as the open-shell singlet state of α,3-didehydrotoluene (**4**), was the only intermediate generated by the cyclization, then reaction with methanol might be expected to afford 2-phenylethanol as the principal product. This expectation is based on the homolytic dissociation energy of the C−H bond, which is 8.5 kcal/mol less than that of the O−H bond in methanol.[4] In accord with this thermodynamic argument, Jones and Bergman demonstrated that 1,4-didehydrobenzene abstracts only the methyl hydrogen from methanol at 200 °C (Figure 3).[5] The question that has been of interest since its first discovery is the origin of the principal product of the title reaction, benzylmethyl ether.

Mechanisms A and B: A Single Intermediate or Rapidly Equilibrating Intermediates? Myers et al. proposed that a resonance structure of the biradical, the closed-shell zwitterionic electronic representation of α,3-didehyrotoluene (**5**), could explain the net O−H insertion product. Their studies showed that the yield of the net O−H insertion product increased with increasing polarity of the medium, consistent with its formation deriving from a polar intermediate. For example, pyrolysis of enyneallene in methanol containing 5.6 M water increased the yield of benzylmethyl ether to 47% from 38% in neat methanol.

By pyrolyzing enyneallene with various isotopomers of methanol, they ruled out two cascade mechanisms: one in which the initially formed biradical intermediate irreversibly decays to a polar intermediate and the other in which the initially formed polar intermediate irreversibly decays to the biradical (Figure 4). These studies also ruled out a mechanism in which enyneallene cyclizes to two noninterconverting intermediates (Figure 4).

Myers et al. determined the rate of disappearance of enyneallene at 75 °C in 1,4-cyclohexadiene to be $(3.8 \pm 0.2) \times 10^{-4}$ s^{-1} and in CD_3OH to be $(4.0 \pm 0.2) \times 10^{-4}$ s^{-1}. Because these rate constants are the same within experimental error, the radical and polar pathways apparently share a common rate-determining step. This result and the above isotope experiments led the

[†] Current address: Department of Chemistry, The Scripps Research Institute, 10550 North Torrey Pines Road, La Jolla, California 92037.

[‡] Current address: Department of Chemistry, The University of Vermont, Cook Physical Sciences Building, 82 University Place, Burlington, Vermont 05405.

(1) Myers, A. G. *Tetrahedron Lett.* **1987**, *28*, 4493.
(2) Reviews: (a) Nicolaou, K. C.; Dai, W.-M. *Angew. Chem., Int. Ed. Engl.* **1991**, *30*, 1387. (b) Grissom, J. W.; Gunawardena, G. U.; Klingberg, D.; Huang, D. *Tetrahedron* **1996**, *52*, 6453.
(3) (a) Myers, A. G.; Kuo, E. Y.; Finney, N. S. *J. Am. Chem. Soc.* **1989**, *111*, 8057. (b) Myers, A. G.; Dragovich, P. S.; Kuo, E. Y. *J. Am. Chem. Soc.* **1992**, *114*, 9369.
(4) Berkowitz, J.; Ellison, G. B.; Gutman, D. *J. Phys. Chem.* **1994**, *98*, 2744.
(5) (a) Jones, R. R.; Bergman, R. G. *J. Am. Chem. Soc.* **1972**, *94*, 660. (b) Bergman, R. G. *Acc. Chem. Res.* **1973**, *6*, 25. (c) Jones, R. R. Ph.D. Dissertation, California Institute of Technology, 1976.

10.1021/ja0445443 CCC: $30.25

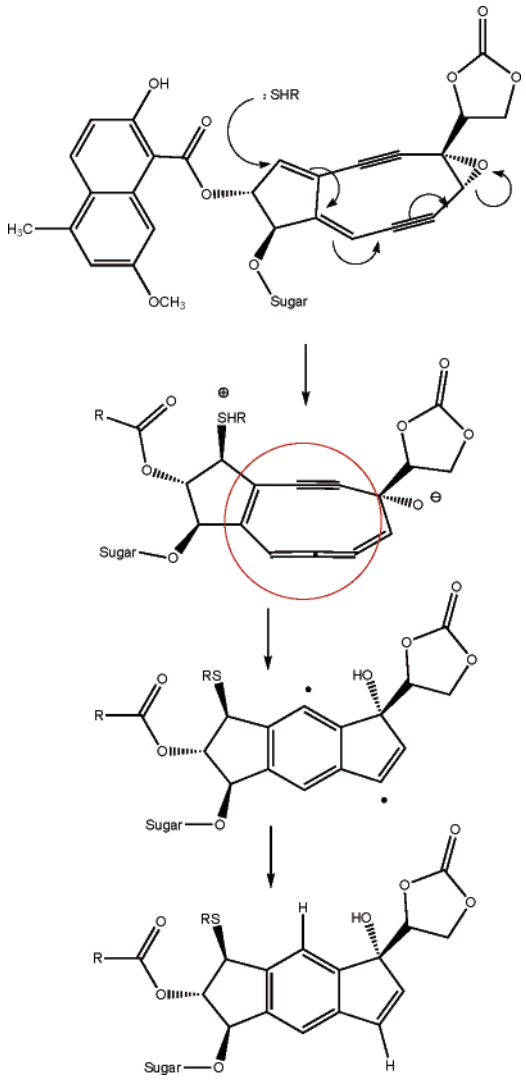

Figure 1. Neocarzinostatin: the proposed mechanism, the enynecumulene core, and a biradical intermediate.[1]

authors to propose a mechanism in which a single intermediate or a pair of rapidly equilibrating intermediates afford the benzylmethyl ether and 2-phenylethanol products (mechanisms **A** and **B**, respectively, in Figure 5).

We have previously pointed out that resonance between the biradical and zwitterionic configurations of α,3-didehydrotoluene is symmetry forbidden (Figure 6).[6−8] A single-intermediate mechanism, where the biradical and zwitterion are in resonance, has also been ruled out experimentally.[7] Mechanism **A** in Figure 5 would predict an invariant product ratio (benzylmethyl ether:2-phenylethanol) in response to an external trap for the biradical, provided that addition of the trap does not significantly alter the system, for example, by changing the solvent polarity. The equilibrating-intermediates mechanism (**B** in Figure 5) leads to the same prediction. However, pyrolysis of enyneallene **1** in methanol with low concentrations of 1,4-cyclohexadiene (0−0.2 M), a trap for the biradical, resulted in a linear increase in the product ratio (benzylmethyl ether:2-phenylethanol) with respect to cyclohexadiene concentration. Above 0.2 M cyclohexadiene, the product ratio started to

(6) Salem, R.; Rowland, C. *Angew. Chem., Int. Ed. Engl.* **1972**, *11*, 92.
(7) Hughes, T. S.; Carpenter, B. K. *J. Chem. Soc., Perkin Trans. 2* **1999**, 2291.
(8) Hughes, T. S. Ph.D. Dissertation, Cornell University, 2000.

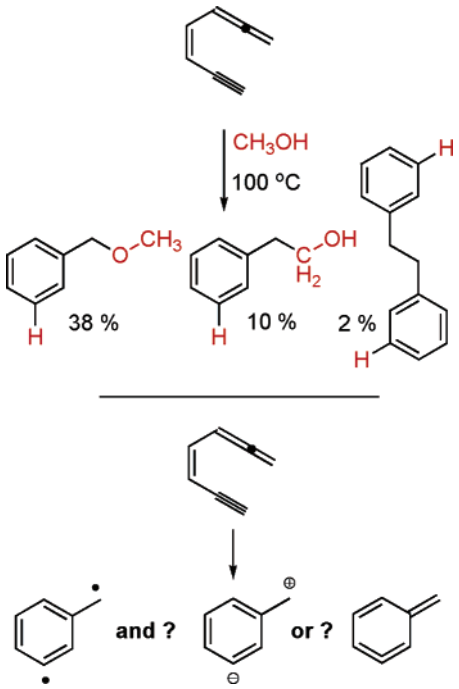

Figure 2. Pyrolysis of enyneallene: Myers et al. observed C−H and O−H insertion products.[3]

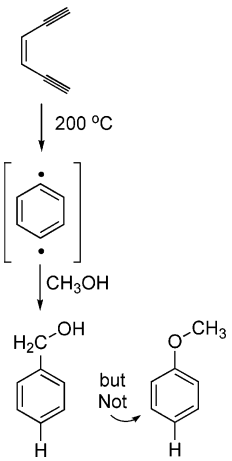

Figure 3. The Bergman cyclization: only C−H insertion (ref 5).

decrease again, consistent with a disfavoring of the polar pathway due to a reduction in solvent polarity.[7] These results ruled out mechanisms **A** and **B** (Figure 5). However, they were consistent with a mechanism in which two intermediates were formed directly from the reactant. The similar rate constants for the disappearance of enyneallene in 1,4-cyclohexadiene and CD_3OH suggest that a common rate-determining step is shared for the radical and polar pathways.[3] Together, the data support a mechanism in which a post-rate-determining bifurcation leads to the radical and polar pathways.

Mechanism C: A Cyclic Allene Intermediate? This conclusion does not uniquely identify the nature of the intermediate involved in the polar mechanism. The polar intermediate could be the zwitterion or a cyclic allene (methylene-1,2,4-cyclohexatriene, **6**), Figure 7.

As described previously, **6** was considered as a possible alternative to the zwitterion for the identity of the polar intermediate.[7] Two strained allenes analogous to **6** are 1,2,4-cyclohexatriene and 1,2,4,6-cycloheptatetraene. Diels−Alder

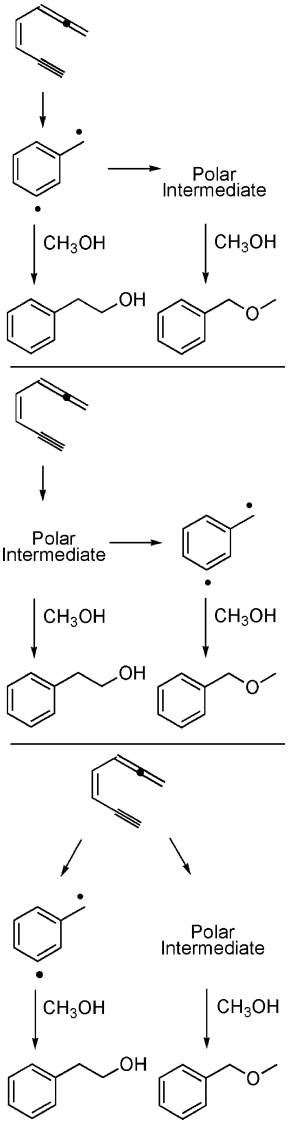

Figure 4. Mechanisms ruled out by Myers et al. (ref 3).

trapping products have been observed for both of these molecules,[9,10] and computational studies show them to be local minima at various levels of theory.[11,12] However, attempts to trap cyclic allene (**6**) by cyclizing enyneallene in the presence of 1,3-cyclopentadiene only resulted in adducts derived from

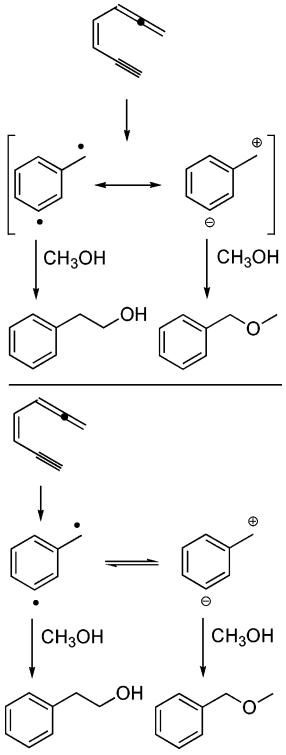

Figure 5. Mechanisms proposed by Myers et al. (ref 3).

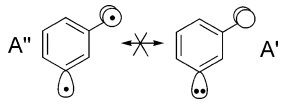

Figure 6. Symmetry forbidden resonance. Biradical **4** is heterosymmetric. The σ-type orbital has A′ symmetry within C_S, while the π-type orbital has A″ symmetry. The $\sigma^1\pi^1$ biradical configuration has A″ symmetry, while the $\sigma^2\pi^0$ zwitterionic configuration has A′ symmetry. The mixing of these electronic configurations is symmetry forbidden.

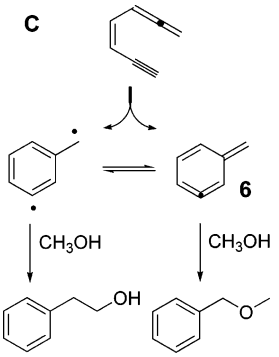

Figure 7. A possible cyclic allene **6** as the intermediate responsible for benzylmethyl ether (ref 7).

reaction with the biradical.[7] This result led to a more thorough computational investigation of the cyclic allene at the CAS-(8,8) level. Repeated attempts to optimize the geometry of this species, with various starting points and with basis sets up to 6-311G(d), led invariably to the biradical minimum.[13] A stability analysis of the cyclic allene from the RHF and RB3LYP levels of theory demonstrated that the restricted wave functions were unstable. Hence, both the computational and experimental results suggest that the cyclic allene (**6**) does not exist as a trappable intermediate.

(9) (a) Hopf, H.; Musso, H. *Angew. Chem., Int. Ed. Engl.* **1969**, *8*, 680. (b) Christl, M.; Braun, M.; Müller, G. *Angew. Chem., Int. Ed. Engl.* **1992**, *31*, 473. (c) Hopf, H.; Berger, H.; Zimmermann, G.; Nüchter, U.; Jones, P. G.; Dix, I. *Angew. Chem., Int. Ed. Engl.* **1997**, *36*, 1187. (d) Christl, M.; Groetsch, S. *Eur. J. Org. Chem.* **2000**, 1871. (e) Zimmermann, G. *Eur. J. Org. Chem.* **2001**, 457.

(10) Harris, J. W.; Jones, W. M. *J. Am. Chem. Soc.* **1982**, *104*, 7329.

(11) (a) Schreiner, P. R.; Karney, W. L.; Schleyer, P. v. R.; Borden, W. T.; Hamilton, T. P.; Schaefer, H. F., III. *J. Org. Chem.* **1996**, *61*, 7030. (b) Wentrup, C.; Wong, M. W. *J. Org. Chem.* **1996**, *61*, 7022. (c) Matzinger, S.; Bally, T.; Patterson, E. V.; McMahon, R. J. *J. Am. Chem. Soc.* **1996**, *118*, 1535.

(12) (a) Engels, B.; Schoneboom, J. C.; Munster, A. F.; Groetsch, S.; Christl, M. *J. Am. Chem. Soc.* **2002**, *124*, 287. See also: (b) Ananikov, V. P. *J. Phys. Org. Chem.* **2001**, *14*, 109. (c) Bettinger, H. F.; Schreiner, P. R.; Schaefer, H. F., III; Schleyer, P. v. R. *J. Am. Chem. Soc.* **1998**, *120*, 5741. (d) Li, Z.; Rogers, D. W.; McLafferty, F. J.; Mandziuk, M.; Podosenin, A. V. *J. Phys. Chem. A* **1999**, *103*, 426. (e) Burrell, R. C.; Daoust, K. J.; Bradley, A. Z.; DiRico, K. J.; Johnson, R. P. *J. Am. Chem. Soc.* **1996**, *118*, 4218. (f) Zahradnik, R.; Hobza, P.; Burcl, R.; Andes H. B., Jr.; Radziszewski, J. G. *THEOCHEM* **1994**, *119*, 335. (g) Sander, W.; Exner, M.; Winkler, M.; Balster, A.; Hjerpe, A.; Kraka, E.; Cremer, D. *J. Am. Chem. Soc.* **2002**, *124*, 13072. (h) Rodriguez, D.; Navarro-Vazquez, A.; Castedo, L.; Dominguez, D.; Saa, C. *J. Org. Chem.* **2003**, *68*, 1938.

(13) Cremeens, M. E.; Carpenter, B. K. *Org. Lett.* **2004**, *6*, 2349.

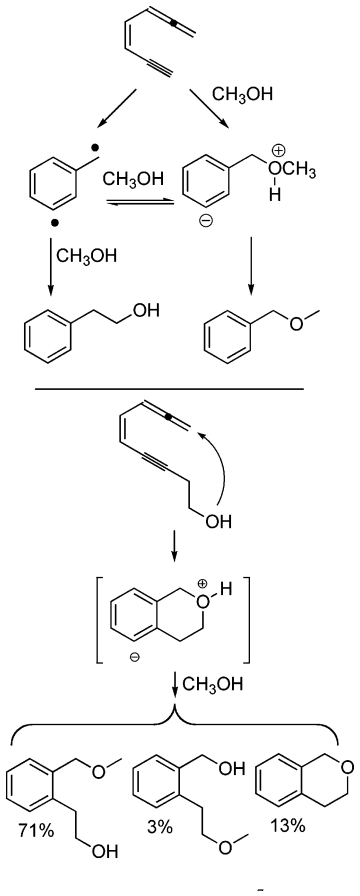

Figure 8. Top: Possible nucleophile-assisted cyclization.[7] Bottom: Intramolecular trapping study. Radical-derived products (4%) were also observed.

Alternatively, if one treated the apparent medium independence of the rate constant for enyneallene cyclization as coincidental, then a methanol-assisted cyclization could be considered as a mechanism for formation of the ether product (mechanism **D**, Figure 8). Intramolecular trapping studies of an enyneallene substituted with a tether capable of participating in either a net C−H or a net O−H insertion pathway supported that possibility (Figure 8).

Methods

Computational. General. The Gaussian 98 and Gaussian 03 program suites[14,15] were used for all restricted (R) and unrestricted (U) single-reference calculations, that is, Hartree−Fock[16] (RHF and UHF) and Becke's three parameter hybrid functional[17] with the Lee−Yang−Parr correlation functional[18] (RB3LYP and UB3LYP). All calculations used the 6-31G(d) basis set, unless stated otherwise. The stabilities of restricted wave functions were checked according to the procedure provided in the Gaussian program.[19] The implicit solvation models[20] used in this work were the polarized continuum model (PCM)[21] and the Onsager model[22] using a dielectric constant of 32.63 for methanol. Analytic harmonic frequencies were used for HF, B3LYP, and CASSCF(8,8) methods, while numeric harmonic frequencies were used for CASSCF methods above an (8,8) active space. All thermal corrections were calculated at 298.15 K, 1 atm, and used unscaled frequencies.

CASSCF, CASPT2, and RS2C. Complete active space self-consistent field (CAS) calculations[23,24] were carried out with the Gaussian 98,[14] Gaussian 03,[15] GAMESS,[25] and MOLPRO[26] programs. The CAS(8,8) calculations on the biradical and zwitterion configurations of α,3-didehydrotoluene employed an active space including three bonding and three antibonding π orbitals, one nonbonding π-type orbital, and one nonbonding σ-type orbital. The active space for CAS-

(14) Frisch, M. J.; Trucks, G. W.; Schlegel, H. B.; Scuseria, G. E.; Robb, M. A.; Cheeseman, J. R.; Zakrzewski, V. G.; Montgomery, J. A., Jr.; Stratmann, R. E.; Burant, J. C.; Dapprich, S.; Millam, J. M.; Daniels, A. D.; Kudin, K. N.; Strain, M. C.; Farkas, O.; Tomasi, J.; Barone, V.; Cossi, M.; Cammi, R.; Mennucci, B.; Pomelli, C.; Adamo, C.; Clifford, S.; Ochterski, J.; Petersson, G. A.; Ayala, P. Y.; Cui, Q.; Morokuma, K.; Malick, D. K.; Rabuck, A. D.; Raghavachari, K.; Foresman, J. B.; Cioslowski, J.; Ortiz, J. V.; Baboul, A. G.; Stefanov, B. B.; Liu, G.; Liashenko, A.; Piskorz, P.; Komaromi, I.; Gomperts, R.; Martin, R. L.; Fox, D. J.; Keith, T.; Al-Laham, M. A.; Peng, C. Y.; Nanayakkara, A.; Challacombe, M.; Gill, P. M. W.; Johnson, B.; Chen, W.; Wong, M. W.; Andres, J. L.; Gonzalez, C.; Head-Gordon, M.; Replogle, E. S.; Pople, J. A. *Gaussian 98*, revision A.9; Gaussian, Inc.: Pittsburgh, PA, 1998.

(15) Frisch, M. J.; Trucks, G. W.; Schlegel, H. B.; Scuseria, G. E.; Robb, M. A.; Cheeseman, J. R.; Montgomery, J. A., Jr.; Vreven, T., Jr.; Kudin, K. N.; Burant, J. C.; Millam, J. M.; Iyengar, S. S.; Tomasi, J.; Barone, V.; Mennucci, B.; Cossi, M.; Scalmani, G.; Rega, N.; Petersson, G. A.; Nakatsuji, H.; Hada, M.; Ehara, M.; Toyota, K.; Fukuda, R.; Hasegawa, J.; Ishida, M.; Nakajima, T.; Honda, Y.; Kitao, O.; Nakai, H.; Klene, M.; Li, X.; Knox, J. E.; Hratchian, H. P.; Cross, J. B.; Adamo, C.; Jaramillo, J.; Gomperts, R.; Stratmann, R. E.; Yazyev, O.; Austin, A. J.; Cammi, R.; Pomelli, C.; Ochterski, J. W.; Ayala, P. Y.; Morokuma, K.; Voth, G. A.; Salvador, P.; Dannenberg, J. J.; Zakrzewski, V. G.; Dapprich, S.; Daniels, A. D.; Strain, M. C.; Farkas, O.; Malick, D. K.; Rabuck, A. D.; Raghavachari, K.; Foresman, J. B.; Ortiz, J. V.; Cui, Q.; Baboul, A. G.; Clifford, S.; Cioslowski, J.; Stefanov, B. B.; Liu, G.; Liashenko, A.; Piskorz, P.; Komaromi, I.; Martin, R. L.; Fox, D. J.; Keith, T.; Al-Laham, M. A.; Peng, C. Y.; Nanayakkara, A.; Challacombe, M.; Gill, P. M. W.; Johnson, B.; Chen, W.; Wong, M. W.; Gonzalez, C.; Pople, J. A. *Gaussian 03*, revision B.05; Gaussian, Inc.: Pittsburgh, PA, 2003.

(16) (a) Roothaan, C. C. J. *Rev. Mod. Phys.* **1951**, *23*, 69. (b) Pople, J. A.; Nesbet, R. K. *J. Chem. Phys.* **1954**, *22*, 571. (c) McWeeny, R.; Dierksen, G. *J. Chem. Phys.* **1968**, *49*, 4852.

(17) Becke, A. D. *J. Chem. Phys.* **1993**, *98*, 5648.

(18) (a) Lee, C.; Yang, W.; Parr, R. G. *Phys. Rev. B* **1988**, *37*, 785. (b) Miehlich, B.; Savin, A.; Stoll, H.; Preuss, H. *Chem. Phys. Lett.* **1989**, *157*, 200.

(19) (a) Seeger, R.; Pople, J. A. *J. Chem. Phys.* **1977**, *66*, 3045. (b) Bauernschmitt, R.; Ahlrichs, R. *J. Chem. Phys.* **1996**, *104*, 9047. (c) Foresman, J. B.; Frisch, Æ. *Exploring Chemistry with Electronic Structure Methods*, 2nd ed.; Gaussian Inc.: Pittsburgh, PA, 1996; Chapter 2. (d) Frisch, Æ.; Frisch, M. J. *Gaussian 98 User's Reference*, 2nd ed.; Manual Rev. 6.1. Gaussian Inc.: Pittsburgh, PA, 1999; p 178.

(20) For an introduction: Cramer, C. J. *Essentials of Computational Chemistry: Theories and Models*; John Wiley & Sons: New York, 2002; Chapter 11.

(21) (a) Miertus, S.; Scrocco, E.; Tomasi, J. *Chem. Phys.* **1981**, *55*, 117. (b) Miertus, S.; Tomasi, J. *Chem. Phys.* **1982**, *65*, 239. (c) Cossi, M.; Barone, V.; Cammi, R.; Tomasi, J. *Chem. Phys. Lett.* **1996**, *255*, 327. (d) Mennucci, B.; Tomasi, J. *J. Chem. Phys.* **1997**, *106*, 5151. (e) Mennucci, B.; Cancès, E.; Tomasi, J. *J. Phys. Chem. B* **1997**, *101*, 10506. (f) Cammi, R.; Mennucci, B.; Tomasi, J. *J. Phys. Chem. A* **1999**, *103*, 9100. (g) Cossi, M.; Barone, V.; Robb, M. A. *J. Chem. Phys.* **1999**, *111*, 5295. (h) Cammi, R.; Mennucci, B.; Tomasi, J. *J. Phys. Chem. A* **2000**, *104*, 5631. (i) Cossi, M.; Barone, V. *J. Chem. Phys.* **2000**, *112*, 2427. (j) Cossi, M.; Barone, V. *J. Chem. Phys.* **2001**, *115*, 4708. (k) Cossi, M.; Rega, N.; Scalmani, G.; Barone, V. *J. Chem. Phys.* **2001**, *114*, 5691. (l) Cossi, M.; Scalmani, G.; Rega, N.; Barone, V. *J. Chem. Phys.* **2002**, *117*, 43. (m) Cossi, M.; Rega, N.; Scalmani, G.; Barone, V. *J. Comput. Chem.* **2003**, *24*, 669.

(22) (a) Onsager, L. *J. Am. Chem. Soc.* **1936**, *58*, 1486. (b) Kirkwood, J. G. *J. Chem. Phys.* **1934**, *2*, 351. (c) Wong, M. W.; Frisch, M. J.; Wiberg, K. B. *J. Am. Chem. Soc.* **1991**, *113*, 4776. (d) Wong, M. W.; Wiberg, K. B.; Frisch, M. J. *J. Am. Chem. Soc.* **1992**, *114*, 523. (e) Wong, M. W.; Wiberg, K. B.; Frisch, M. J. *J. Chem. Phys.* **1991**, *95*, 8991. (f) Wong, M. W.; Wiberg, K. B.; Frisch, M. J. *J. Am. Chem. Soc.* **1992**, *114*, 1645.

(23) (a) Roos, B. O.; Taylor, P. R.; Siegbahn, P. E. M. *Chem. Phys.* **1980**, *48*, 157. (b) Hegarty, D.; Robb, M. A. *Mol. Phys.* **1979**, *38*, 1795. (c) Eade, R. H. E.; Robb, M. A. *Chem. Phys. Lett.* **1981**, *83*, 362. (d) Schlegel, H. B.; Robb, M. A. *Chem. Phys. Lett.* **1982**, *93*, 43. (e) Bernardi, F.; Bottini, A.; McDougall, J. J. W.; Robb, M. A.; Schlegel, H. B. *Faraday Symp. Chem. Soc.* **1984**, *19*, 137. (f) Yamamoto, N.; Vreven, T.; Robb, M. A.; Frisch, M. J.; Schlegel, H. B. *Chem. Phys. Lett.* **1996**, *250*, 373. (g) Frisch, M. J.; Ragazos, I. N.; Robb, M. A.; Schlegel, H. B. *Chem. Phys. Lett.* **1992**, *189*, 524.

(24) Some CAS reviews: (a) Schmidt, M. W.; Gordon, M. S. *Annu. Rev. Phys. Chem.* **1998**, *49*, 233. (b) Roos, B. O. In *Advances in Chemical Physics*; Lawley, K. P., Ed.; Wiley Interscience: New York, 1987; Vol. 69, pp 339−445. (c) Shepard, R. *Adv. Chem. Phys.* **1987**, *69*, 63.

(25) Schmidt, M. W.; Baldridge, K. K.; Boatz, J. A.; Elbert, S. T.; Gordon, M. S.; Jensen, J. J.; Koseki, S.; Matsunaga, N.; Nguyen, K. A.; Su, S.; Windus, T. L.; Dupuis, M.; Montgomery, J. A. *J. Comput. Chem.* **1993**, *14*, 1347.

(26) *MOLPRO*, version 2002.3; Amos, R. D.; Bernhardsson, A.; Berning, A.; Celani, P.; Cooper, D. L.; Deegan, M. J. O.; Dobbyn, A. J.; Eckert, F.; Hampel, C.; Hetzer, G.; Knowles, P. J.; Korona, T.; Lindh, R.; Lloyd, A. W.; McNicholas, S. J.; Manby, F. R.; Meyer, W.; Mura, M. E.; Nicklass, A.; Palmieri, P.; Pitzer, R.; Rauhut, G.; Schütz, M.; Schumann, U.; Stoll, H.; Stone, A. J.; Tarroni, R.; Thorsteinsson, T.; Werner, H.-J.

(10,10) calculations included the orbital set just described plus the bonding and antibonding σ orbital between the C1 and C2 carbons of the α,3-didehydrotoluene framework, which corresponds to the bond that forms during the cyclization of the enyneallene. For the CAS-(10,10) active space of the enyneallene, five bonding and five antibonding π orbitals were used.

Single-point second-order perturbation theory calculations[27] were used to account for dynamic electron correlation corrections to the CAS wave functions, although it is noted that this method suffers from a systematic error when the number of paired electrons changes between species.[28] The CASPT2 method that is employed by Andersson et al. underestimates the electron pairing process by about 3−6 kcal/mol. In the context of this work, the implication is that the energy difference between the biradical and zwitterion at the CASPT2(8,8)//CAS(8,8) level of theory, where the number of paired electrons changes, would overestimate this energy difference by 3−6 kcal/mol. Unless otherwise noted, the variant of CASPT2 employed here was the one available in MOLPRO referred to as RS2C for Rayleigh−Schrödinger perturbation theory,[29] which presumably suffers from the same systematic error. RS2C is a multireference second-order perturbation theory computational method very similar to the commonly employed CASPT2 method of Andersson et al. For example, the CASPT2(8,8)/6-31G(d) energy of the CAS(8,8)/6-31G(d) biradical is −269.3609900 hartrees where the RS2C(8,8)/6-31G(d) energy is −269.3614115 hartrees, and the difference is only 0.4 millihartree (0.26 kcal/mol). All conical intersection searches were performed in MOLPRO. State-averaged (SA) calculations were performed primarily with the GAMESS program, but on occasion performed with MOLPRO or Gaussian.

B3LYP. Although the calculation of triplet biradicals with an unrestricted single-reference wave function is a standard procedure,[30] the representation of singlet biradicals with an unrestricted single-reference wave function has been questioned.[31] Nevertheless, unrestricted single-reference DFT calculations are frequently performed on singlet biradicals because they can give reasonable results.[32−34] By using a triplet wave function as an initial guess for optimizing a singlet biradical, one arrives at the lowest energy singlet biradical wave function. For example, at the UB3LYP/6-31G(d) level, the singlet−triplet energy gap of α,3-didehydrotoluene was found to be −1.2 kcal/mol, which is similar to the DDCI2/6-31G(d,p) (−2.1 kcal/mol),[35] MCSCF(8,8)/pVDZ//MCSCF(8,8)/3-21G (−3.0 kcal/mol),[36] CASSCF-(8,8)/6-31G(d,p)//ROSS-B3LYP/6-31G(d,p) (−3.0 kcal/mol),[37] MR-CI+Q (0.0 kcal/mol),[34] BLYP/6-31G(d) (−0.6 kcal/mol),[38] and experimental (−5 to 0 kcal/mol)[39] estimates. Modeling the first singlet excited state of α,3-didehydrotoluene, the zwitterion, with a spin-restricted single reference computational method under a C_S symmetry constraint can be justified because this state is dominated by a closed-shell single configuration.

To approximate vertical excitation energies, time-dependent (TD) DFT was employed.[40,41] The use of TDB3LYP for vertical excitation energies has been reviewed and shown to give reasonable results when the excitation is less than one-half of the ionization potential.[41] With respect to excitations from the ground state of nonequilibrium geometries, this method was found to qualitatively reproduce multi-reference results.[42] One technical challenge in using unrestricted single-reference methods to calculate singlet biradicals is determining the lowest energy wave function. The validity of the spin-contaminated wave functions for singlet biradicals from the UB3LYP method was evaluated by the TDUB3LYP method; *negative* vertical excitation energies resulted from wave functions that did not have the lowest energy. Consequently, it was presumed that the lowest energy, spin-contaminated, singlet wave function was reached if TDUB3LYP predicted only positive vertical excitation energies.

Experimental

General. Nuclear magnetic resonance (NMR) was performed with a Varian XL 200 MHz spectrometer, a Bruker AF 300 MHz spectrometer, an INOVA 400 MHz spectrometer, or a Varian Unity 500 MHz spectrometer. The spectra in $CDCl_3$ were referenced to $CHCl_3$ (7.26 ppm), and those in C_6D_6 were referenced to C_6D_5H (7.16 ppm). Infrared (IR) spectra were acquired with a Nicolet Impact 410 FT-IR spectrometer as a neat solution on KBr plates, and absorptions were identified as strong (s), medium (m), or weak (w). Analytical gas chromatography (GC) was accomplished with a Hewlett-Packard 6890 GC equipped with a flame ionization detector (FID) and an HP1 capillary column (dimethylsiloxane, 30 m × 0.32 mm × 0.25 μm). Injection volumes were routinely 2−3 μL. The oven temperature was 35 °C for 5 min, increased to 255 °C over 22 min, and held at 255 °C for 5 min. The detector temperature was set to 275 °C. The injector temperature was set to 150 °C for routine use and was set to 100 °C when analyzing enyneallene. Injections were split at a ratio of 20:1. Helium was the carrier gas with a flow rate of 2.3 mL/min. Mass spectra were acquired with a Hewlett-Packard 5890 GC coupled to a Hewlett-Packard 5970 Mass Selective Detector. The ionization potential was left to its default value of 70 eV. The capillary column was a DB1 (dimethylsiloxane, 30 m × 0.25 mm × 0.25 μm). The oven temperature was 35 °C for 5 min, increased to 255 °C over 22 min, and held at 255 °C for 5 min. The detector temperature was set to 275 °C. The injector temperature was set to 100 °C. Injections were split with a split ratio of 1:1. Helium was the carrier gas with a flow rate of 1 mL/min.

Nona-5,7,8-trien-3-yn-1-ol Acetate. A quantity of 0.64 mL (4.04 mmol, 1.30 equiv) of diethylazodicarboxylate was added dropwise via syringe to a stirred, ice-cooled solution of 1.06 g (4.13 mmol, 1.33 equiv) of triphenylphosphine in 15 mL of tetrahydrofuran. After being stirred under nitrogen at 0 °C for 15 min, a solution of 0.60 g (3.12 mmol, 1.00 equiv) of non-4-en-2,6-diyn-1,9-diol 9-acetate[43] in 10 mL of tetrahydrofuran was added. After an additional 15 min, a solution of 0.80 g (3.68 mmol, 1.18 equiv) of *o*-nitrobenzenesulfonhydrazide in 10 mL of tetrahydrofuran was added. The solution was stirred for an additional 4 h at 0 °C, then allowed to warm to room temperature. After 24 h, the reaction mixture was concentrated in vacuo, and the resultant orange oil was triturated with pentane. The remaining oil was purified by column chromatography to yield, along with the concentrated pentane washings, 0.44 g of yellow oil (80.0% yield). IR (neat

(27) Andersson, K.; Malmqvist, P.; Roos, B. O. *J. Chem. Phys.* **1992**, *96*, 1218.
(28) Andersson, K.; Roos, B. O. *Int. J. Quantum Chem.* **1993**, *45*, 591.
(29) Celani, P.; Werner, H. J. *J. Chem. Phys.* **2000**, *112*, 5546.
(30) Bally, T.; Borden, W. T. In *Reviews in Computational Chemistry*; Lipkowitz, K. B., Boyd, D. B., Eds.; Wiley-VCH: New York, 1999; Vol. 13, pp 1−98. Given $\langle S^2\rangle = s(s+1)$, where s is the maximum value of $\langle S_Z\rangle$, for a triplet $\langle S^2\rangle = 2.0$ because $\langle S_Z\rangle = +1$, 0, −1 and $s = 1$. For a singlet, $\langle S^2\rangle = 0$ because $\langle S_Z\rangle = 0$ and $s = 0$. For a doublet, $\langle S^2\rangle = 0.75$ because $\langle S_Z\rangle = +1/2$, $-1/2$, and $s = +1/2$.
(31) (a) Grafenstein, J.; Cremer, D. *Mol. Phys.* **2001**, *99*, 981. (b) Orlova, G.; Goddard, J. D. *J. Chem. Phys.* **2000**, *112*, 10085. (c) Staroverov, V. N.; Davidson, E. R. *J. Am. Chem. Soc.* **2000**, *122*, 186. (d) Wittbrodt, J. M.; Schlegel, H. B. *J. Chem. Phys.* **1996**, *105*, 6574. (e) Yamaguchi, K.; Jensen, F.; Dorigo, A.; Houk, K. N. *Chem. Phys. Lett.* **1988**, *149*, 537.
(32) (a) Beno, B. R.; Wilsey, S.; Houk, K. N. *J. Am. Chem. Soc.* **1999**, *121*, 4816. (b) Goldstein, E.; Beno, B.; Houk, K. N. *J. Am. Chem. Soc.* **1996**, *118*, 6036. (c) Houk, K. N.; Beno, B. R.; Nendel, M.; Black, K.; Yoo, H. Y.; Wilsey, S.; Lee, J. *THEOCHEM* **1997**, *398*−*399*, 169.
(33) (a) Cramer, C. J. *J. Am. Chem. Soc.* **1998**, *120*, 6261. (b) Cramer, C. J.; Smith, B. A. *J. Phys. Chem.* **1996**, *100*, 9664. (c) Grafenstein, J.; Kraka, E.; Filatov, M.; Cremer, D. *Int. J. Mol. Sci.* **2002**, *3*, 360. (d) Cremer, D. *Mol. Phys.* **2001**, *99*, 1899.
(34) Engels, B.; Hanrath, M. *J. Am. Chem. Soc.* **1998**, *120*, 6356.
(35) Cabrero, J.; Ben-Amor, N.; Caballol, R. *J. Phys. Chem. A* **1999**, *103*, 6220.
(36) Wenthold, P. G.; Wierschke, S. G.; Nash, J. J.; Squires, R. R. *J. Am. Chem. Soc.* **1993**, *115*, 12611.
(37) Grafenstein, J.; Cremer, D. *Phys. Chem. Chem. Phys.* **2000**, *2*, 6220.
(38) (a) Prall, M.; Wittkopp, A.; Schreiner, P. R. *J. Phys. Chem. A* **2001**, *105*, 9265. (b) Schreiner, P. R.; Prall, M. *J. Am. Chem. Soc.* **1999**, *121*, 8615.
(39) Logan, C. F.; Ma, J. C.; Chen, P. *J. Am. Chem. Soc.* **1994**, *116*, 2137.
(40) (a) Stratmann, R. E.; Scuseria, G. E.; Frisch, M. J. *J. Chem. Phys.* **1998**, *109*, 8218. (b) Casida, M. E.; Jamorski, C.; Casida, K. C.; Salahub, D. R. *J. Chem. Phys.* **1998**, *108*, 4439.
(41) Bauernschmitt, R.; Ahlrichs, R. *Chem. Phys. Lett.* **1996**, *256*, 454.
(42) (a) Furche, F.; Ahlrichs, R. *J. Chem. Phys.* **2002**, *117*, 7433. (b) Fantacci, S.; Migani, A.; Olivucci, M. *J. Phys. Chem. A* **2004**, *108*, 1208.
(43) Nagata, R.; Yamanaka, H.; Murahashi, E.; Saito, I. *Tetrahedron Lett.* **1990**, *31*, 2907.

on KBr): 3036.9 (w), 2961.2 (m), 2914.5 (w), 2254.5 (w), 2215.1 (w), 1933.3 (s), 1740.1 (s), 1385.0 (s), 1364.3 (s), 1238.7 (s), 1043.4 (s), 910.5 (m), 850.7 (m), 732.9 (s). ^{1}H NMR ($CDCl_3$, 300 MHz) δ (ppm): 6.316 (d × t, 1H, J = 11.3, 6.5 Hz), 6.168 (d × d, 1H, J = 10.7, 10.5 Hz), 5.294 (d × t, 1H, J = 10.7, 2.2 Hz), 4.198 (d, 2H, J = 6.5 Hz), 4.146 (t, 2H, J = 7.0 Hz), 2.668 (t × d, 2H, J = 7.0, 2.2 Hz), 2.024 (s, 3H). ^{13}C NMR ($CDCl_3$, 75 MHz) δ (ppm): 213.7, 170.9, 135.4, 108.4, 92.7, 91.5, 78.7, 76.6, 61.4, 24.3, 22.6. ($CDCl_3$ = 77.29) MS (*m*/*z*): 116 (100), 115 (27.4), 117 (12.5), 105 (10.8), 77 (8.1), 103 (5.1), 78 (5.1), 51 (5.0), 63 (4.6), 79 (3.8), 104 (3.5), 91 (3.4).

Nona-5,7,8-trien-3-yn-1-ol. A quantity of 0.44 g (2.50 mmol, 1.00 equiv) of nona-5,7,8-trien-3-yn-1-ol acetate was dissolved in 25 mL of ethanol; 0.07 mL of 2 N aqueous sodium hydroxide was added, and the brown solution was stirred for 2 h. Another 0.18 mL portion of sodium hydroxide was added, and after an additional 90 min of stirring, the reaction mixture was partitioned between water and pentane. The pentane layers were washed with water and dried with sodium sulfate. Concentration and purification by flash column chromatography (10% ethyl acetate in hexanes on silica) gave 0.18 g of yellow oil (52% yield). ^{1}H NMR ($CDCl_3$, 300 MHz) δ (ppm): 6.346 (d × t, 1H, J = 10.7, 6.5 Hz), 6.192 (d × d, 1H, J = 10.7, 10.2 Hz), 5.399 (d × m, 1H, J = 10.2 Hz), 4.943 (d, 2H, J = 6.5 Hz), 3.731 (t, 2H, J = 6.5 Hz), 2.625 (t × d, 2H, J = 6.5, 2.2 Hz), 2.253 (s, 1H). ^{13}C NMR ($CDCl_3$, 75 MHz) δ (ppm): 213.8, 135.3, 108.5, 91.6, 79.0, 76.7, 61.4, 24.3.

Nona-5,7,8-trien-3-yn-1-ol: Pyrolysis in Methanol. Solutions (125 μL) of ~3 mM nona-5,7,8-trien-3-yn-1-ol in CH_3OH were placed in Pyrex glass tubes (4 mm i.d. × 6 mm o.d.), subjected to three freeze−pump−thaw cycles, and sealed under passive vacuum. The sealed tubes were heated at 90.0 °C for 16−20 h. The tubes were then scored, opened, and the contents analyzed by GC−MS and GC−IR. The products were identified by comparison of GC−MS fragmentation patterns, GC−IR spectra, and GC retention times with authentic samples. As controls, isochroman and 2-(2-methoxymethylphenyl)-ethanol were pyrolyzed in the same manner.

Enyneallene: Pyrolysis with Varying Concentrations of Methanol. Solutions (125 μL) of ~3 mM enyneallene, 0.14 mM C_6D_6, and 0.9 mM *o*-xylene-α,α,α,α′,α′,α′-d_6 (*o*-xylene-d_6) in CH_3OH, C_6D_6, and mixtures of CH_3OH and C_6D_6 were placed in Pyrex glass tubes (4 mm i.d. × 6 mm o.d.), subjected to three freeze−pump−thaw cycles, and sealed under passive vacuum. The sealed tubes were placed in a thermostated ethylene glycol bath (90.0 °C) and heated overnight. Both trials used one data point per concentration of methanol in C_6D_6, where the first trial used concentrations of 0.1, 0.5, 1, 5, 10, 15, and 20 M and the second trial used concentrations of 0.5, 1, 5, 10, 15, 20, and 24 M. Tubes were scored, opened, and analyzed by GC.

Enyneallene: Kinetic Studies in Methanol. Solutions (125 μL) of ~3 mM enyneallene, 0.14 mM C_6D_6, and 0.9 mM *o*-xylene-d_6 in CH_3OH, C_6D_6, and a (1:1) mixture of CH_3OH and C_6D_6 were placed in Pyrex glass (4 mm i.d. × 6 mm o.d.) tubes, subjected to three freeze−pump−thaw cycles, and sealed under passive vacuum. The sealed tubes were placed in a thermostated ethylene glycol bath (75.0 °C). Time intervals were ~25 min, and tubes were placed in an ice bath. For the experiment with 12 M CH_3OH in C_6D_6, 62 total tubes were created. After 25.17, 48.20, 73.25, 98.35, and 123.25 min, 13, 12, 12, 12, and 13 tubes, respectively, were extracted from the batch and chilled. For the experiment in neat CH_3OH, 60 total tubes were created. After 25.40, 50.25, 75.38, 100.15, and 125.25 min, 12, 12, 12, 12, and 12 tubes, respectively, were extracted from the batch and chilled. For the experiment with 15 mM CH_3OH in C_6D_6, 44 total tubes were created. After 25.5, 50.5, 75.75, 100.75, and 126.5 min, 7, 8, 9, 9, and 11 tubes, respectively, were extracted from the batch and chilled. Tubes were scored, opened, and analyzed by GC.

Dibenzoyl Peroxide: Photolysis and Pyrolysis in Methanol. Dibenzoyl peroxide (0.023 M) in benzene-d_6 (1.03 M) was photolyzed (high-pressure Hg lamp, Pyrex filter, 21 °C, 2 h) and pyrolyzed (80 °C, 14.5 h) while varying the isotopic labeling of methanol (CH_3OH, CD_3OH, CH_3OD; 22.4 M) in sealed Pyrex tubes that underwent three freeze−pump−thaw cycles. Benzene-d_6 was added to dissolve dibenzoyl peroxide. Tubes were scored, opened, and analyzed by GC−MS.

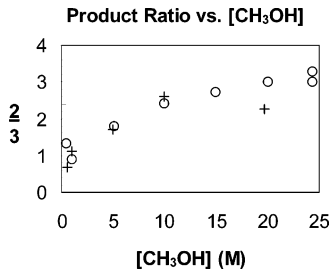

Figure 9. Product ratio versus methanol concentration: enyneallene (~3 mM) was pyrolyzed at 90.0 °C in C_6D_6. Pluses indicate the first trial, and open circles indicate the second trial.

Results and Discussion

Mechanism D: Nucleophile-Assisted Cyclization? The consideration of a nucleophile-promoted cyclization to explain the formation of benzylmethyl ether (Figure 8, **D**) was prompted by the results of an intramolecular trapping study (Figure 8). Nona-5,7,8-trien-3-yn-1-ol, an enyneallene containing a proximally tethered alcohol capable of undergoing intramolecular net C−H and net O−H insertion reactions, was pyrolyzed in methanol. In addition to intra- and intermolecular net C−H insertion products, the intramolecular net O−H insertion product, isochroman (**7**), and the intermolecular net O−H insertion product, **8**, were observed. The observation of **9** in the product mixture seemed to suggest the intermediacy of zwitterion **10** since a control experiment showed that **9** was not formed from **8** or isochroman **7** under the reaction conditions. Intermediate **10** could also be the source of the other two net O−H insertion products. The possibility that **10** was formed directly from the reactant led, in turn, to consideration of the role of methanol in the cyclization of the parent enyneallene, **1**. If methanol promoted the cyclization, it would affect the rate of disappearance of enyneallene. Such an effect would not be detectable when methanol was used as solvent, and so an experiment was devised in which the rate of cyclization could be measured as a function of the concentration of methanol in an inert cosolvent. In order for one to be appreciably confident in any observed changes in the rate of disappearance of the starting material, the ratio of methanol-derived products needs to remain relatively unchanged while the concentration of methanol is varied (for an explanation, see Supporting Information). Benzene-d_6 was chosen as the cosolvent because it was expected to be sufficiently unreactive toward the radical intermediates. An exploratory experiment was run over a large range of methanol concentrations to determine the lowest possible concentration that still afforded a product ratio close to that in neat methanol (Figure 9).

From the results summarized by the graph in Figure 9, it was clear that a methanol concentration below 10 M was unacceptable. Consequently, a concentration of 12 M was chosen as the lower limit for the study. Enyneallene **1** was synthesized as previously reported and was pyrolyzed at 75.0 °C. Its disappearance was followed by GC, using *o*-xylene-d_6 (0.9 mM) as an internal standard. The results for the rate of disappearance of enyneallene are presented in Figure 10 (k_{obs} = (4.43 ± 0.07) × 10^{-4} s^{-1} for 24.4 M CH_3OH; k_{obs} = (5.28 ± 0.10) × 10^{-4}

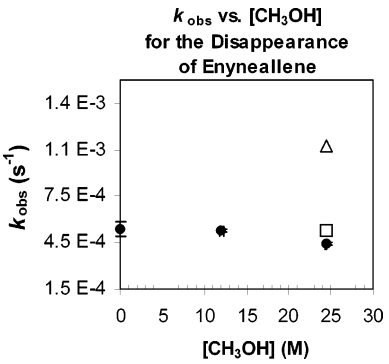

Figure 10. Zeroth-order in methanol: enyneallene (~3 mM) was pyrolyzed at 75.0 °C ($k_{obs} = k[CH_3OH]^a$). Filled circles are the experimental rate constants and include error bars. The predictions, open triangle and box, were based on the experimental k_{obs} at 12 M. The open triangle is the predicted k_{obs} when first-order in methanol ($a = 1$), while the open square is the predicted value for zeroth-order in methanol ($a = 0$).

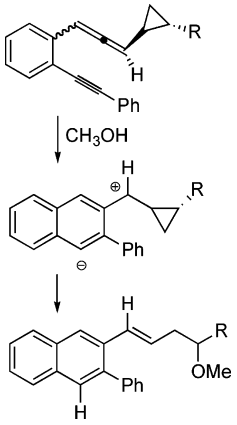

Figure 11. Trapping study by Dopico and Finn where R was *n*-Bu and *i*-Pr (ref 44).

s^{-1} for 12.0 M CH_3OH in C_6D_6; $k_{obs} = (5.38 \pm 0.47) \times 10^{-4}$ s^{-1} for 15 mM CH_3OH in C_6D_6). The reported error is the standard error mean (SEM) at 95% confidence interval for 60, 62, and 44 points, respectively. In Figure 10, the predicted rates for a reaction that is first-order and zeroth-order in methanol (based upon the observed rate constant for 12 M methanol) are plotted for comparison to the experimental result.

Pyrolysis of enyneallene in 15 mM methanol/benzene-d_6 led to unidentified high molecular weight products, but interestingly, the rate constant for disappearance of enyneallene **1** was close to that in 12 M methanol. These results indicated that the rate of disappearance for enyneallene was insensitive to methanol concentration. The graph in Figure 10 shows a zeroth-order dependence in methanol, and therefore, a nucleophile-promoted cyclization is ruled out.

Mechanisms E, F, and G: The Zwitterion as the Second Intermediate. Of the possible intermediates to explain benzyl-methyl ether formation considered to date, the zwitterion **5** is the only one that remains plausible. This proposal is consistent with a study by Dopico and Finn, which showed net O−H insertion for the cyclopropane ring-opened product of substituted enyneallenes (Figure 11).[44] The gas-phase zwitterion is an excited state where the zwitterion−biradical energy difference (ΔE_{elec}) is 39 kcal/mol at the CAS(8,8) level of theory, 31−34 kcal/mol at the CASPT2(8,8) level of theory,[45] and 31 kcal/mol[46] at the B3LYP level of theory. Given these large energy differences, extensive solvent complexation would be required for the zwitterion to be close in energy to the biradical. However, because the disappearance of enyneallene is zeroth-order in methanol, the zwitterion cannot be directly formed in a solvated state.

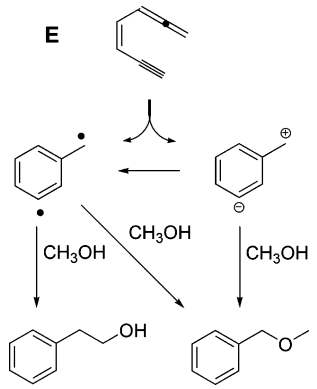

Figure 12. Ether formation by the biradical?

For a zwitterion to be the second intermediate and to be consistent with the 1,4-cyclohexadiene trapping study as well as the isotope studies of Myers et al. cited earlier, one must invoke direct access to the zwitterion from enyneallene. Any mechanism or kinetic expression where the enyneallene is not directly connected to the zwitterion is inconsistent with these results. Additionally, the enyneallene must produce both intermediates after the transition state to be consistent with the lack of dependence on solvent polarity for rate constants observed by Myers et al. for the disappearance of the enyneallene (vide supra). *For this post-rate-determining bifurcation, a surface crossing must occur, which means the reaction must be at least partly nonadiabatic.*

It is perhaps useful to think of the reaction in terms of two crossing diabatic surfaces. One is a closed-shell diabat, leading from the ground electronic state of the reactant to the zwitterionic excited state (**5**) of α,3-didehydrotoluene. The other is an open-shell diabat, leading from a π,π^* excited state of the reactant to the biradical ground state (**4**) of α,3-didehydrotoluene. Mixing of these diabatic surfaces in the C_1 symmetry region of the cyclization leads to the adiabatic representation, in which S_0 is closed-shell at geometries close to the reactant but open-shell at geometries close to the intermediate. To explain the experimental observation, while being consistent with the computed relative energies of the intermediates, it is necessary to propose that the cyclization follow (at least partly) a nonadiabatic course in which the cyclization stays in a closed-shell electronic configuration throughout and thereby generates the zwitterionic intermediate.

There are three plausible mechanisms consistent with these requirements (mechanism **E** in Figure 12 and mechanisms **F** and **G** in Figure 13).[47] Although all three invoke a surface crossing, mechanism **E** can be discussed prior to addressing the proposed surface crossing.

(44) (a) Dopico, P. G.; Finn, M. G. *Tetrahedron* **1999**, *55*, 29. (b) For another example of a net O−H insertion product, see: Toshima, K.; Ohta, K.; Ohtake, T.; Tatsuta, K. *Tetrahedron Lett.* **1991**, *32*, 391.

(45) Note the systematic error with CASPT2 when comparing systems that have different numbers of paired electrons; see ref 28. Consequently, the zwitterion−biradical energy difference would be overestimated by 3−6 kcal/mol, thereby producing a CASPT2 estimate of 31−34 kcal/mol.

(46) Feng, L.; Kumar, D.; Birney, D. M.; Kerwin, S. M. *Org. Lett.* **2004**, *6*, 2059.

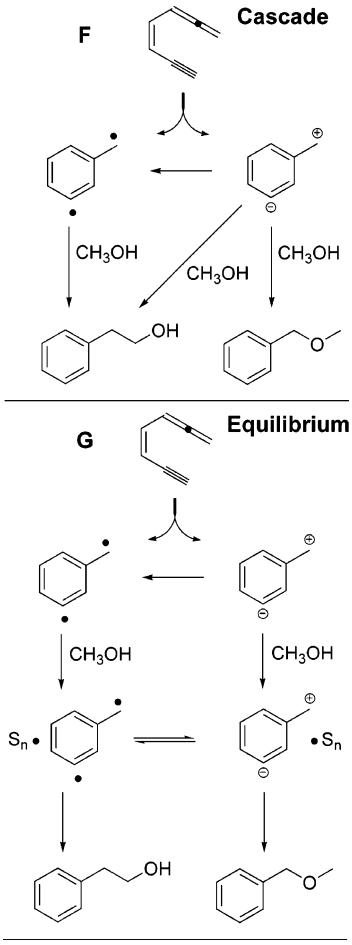

Figure 13. Plausible mechanisms **F** and **G**. S_n represents solvent (i.e., methanol).

Mechanism E: Ether Formation from the Biradical? Although it is an experimental fact that the O−H bond of methanol is 8.5 kcal/mol stronger than the C−H bonds,[4] it has long been known that there is, at best, a weak correlation between bond dissociation energies and reactivities of covalently bound hydrogens toward radical abstraction.[48] One should, therefore, consider the possibility that at least some of the benzylmethyl ether formed from cyclization of enyneallene **1** in methanol arises by reaction of biradical **4** with the hydroxylic hydrogen of the solvent. A variety of calculations on singlet and triplet states of **4** as well as on the phenyl radical as a model for **4** suggested that this was a possibility.[49] For example, CBS-QB3 calculations,[50] which reproduce the experimental C−H and O−H bond dissociation enthalpies of methanol to within 0.5 kcal/mol, show a 1.8 kcal/mol lower activation enthalpy for abstraction of the hydroxylic hydrogen by the phenyl radical. On the other hand, this result stands in contrast to the previously cited report by Bergman in which 1,4-didehydrobenzene was found experimentally to abstract only a C−H hydrogen from methanol.[5]

In an effort to resolve this issue, a phenyl radical was generated both thermally and photochemically from dibenzoyl peroxide in CH_3OD and in CD_3OH solutions. Although these reactions resulted in complex product mixtures, it was possible to analyze the benzene products by mass spectrometry and to show that only the CD_3OH solvent led to formation of C_6H_5D. This apparent disagreement with theory was resolved when calculations using the PCM solvent model for methanol were conducted.[49] These calculations confirmed that *in liquid methanol* C−H abstraction is preferred, as the experiments had shown. Although the PCM model does not include explicit hydrogen bonds, one can, with hindsight, recognize that abstraction of a hydroxylic hydrogen atom in liquid methanol requires breaking *both* the covalent O−H bond *and* a hydrogen bond, whereas the abstraction of a methyl hydrogen atom requires only the covalent C−H bond to be broken. In summary, the earlier experiments of Bergman, the experiments reported here, and the calculations in which solvent effects are included suggest that radicals and biradicals should abstract only a C−H hydrogen from liquid methanol, and that biradical **4** is consequently not a plausible source for benzylmethyl ether. These results rule out mechanism **E** (Figure 12).

Mechanisms F and G: A Possible Nonadiabatic Transition. Because the solution phase experimental results led us to propose the possibility of a nonadiabatic pathway, we chose to explore the gas-phase potential energy (PE) surface for surface crossings, which could lend support to our proposal. If a crossing were found to be energetically accessible in the gas phase, then it would be reasonable to approximate that it could be accessible in the solution phase. For the enyneallene to zwitterion conversion in the gas phase, the transition is from the ground-state singlet surface (S_0) to the first excited-state singlet surface (S_1) and is a nonadiabatic transition. More commonly, the reverse (S_1 to S_0) is proposed and can be accomplished through a radiative or a nonradiative transition.[51] The nonradiative transition, which is relevant to the present case, can occur through vibronic coupling in the vicinity of an avoided crossing or via a conical intersection. The energy gap between the S_0 and S_1 states in the vicinity of the transition structure is large (vide infra), which makes a transition via vibronic coupling unlikely in those regions of the PE surface. The possibility of surface crossing in an alternative part of the PE surface was, therefore, explored by searching for an avoided crossing or conical intersection.[52] Commonly, passage through a conical intersection is invoked only for excited-state to ground-state transitions. However, Atchity et al. showed that passage from the ground state to the excited state is possible,[53] and Blancafort et al. offered an additional discussion on surface crossings.[54] The thermal generation of an excited state has precedent, for

(47) This conclusion resulted from analyzing possible kinetic schemes. It was found that the schemes in Figures 12 and 13 predict the observed linear relationship between the product ratio and concentration of radical trap. Also, these mechanisms are consistent with the isotope experiments of Myers et al., notably, the increase in benzylmethyl ether yield upon pyrolysis of enyneallene in CD_3OH.

(48) (a) Zavitsas, A. A. *J. Am. Chem. Soc.* **1972**, *94*, 2779. (b) Roberts, B. *J. Chem. Soc., Perkin Trans. 2* **1994**, 2155. (c) Shaik, S.; Wu, W.; Dong, K.; Song, L.; Hiberty, P. C. *J. Phys. Chem. A* **2001**, *105*, 8226. (d) Zavitsas, A. A. *J. Phys. Chem. A* **2002**, *106*, 5041.

(49) Borden, W. T.; Hrovat, D.; Isborn, C. Unpublished results, University of Washington, 2003.

(50) Montgomery, J. A., Jr.; Frisch, M. J.; Ochterski, J. W.; Petersson, G. A. *J. Chem. Phys.* **1999**, *110*, 2822.

(51) For an introduction: (a) Klessinger, M.; Michl, J. *Excited States and Photochemistry of Organic Molecules*; VCH: New York, 1995; Sections 4.1.1, 4.1.2, and 5.2. (b) Barltrop, J. A.; Coyle, J. D. *Principles of Photochemistry*; John Wiley & Sons: New York, 1978; Sections 3.1 and 3.3.

(52) Robb, M. A.; Garavelli, M.; Olivucci, M.; Bernardi, F. In *Reviews in Computational Chemistry*; Lipkowitz, K. B., Boyd, D. B., Eds.; Wiley-VCH: New York, 2000; Vol. 15, pp 87−146.

(53) Atchity, G.; Xantheas, S. S.; Ruedenberg, K. *J. Chem. Phys.* **1991**, *95*, 1862.

(54) Blancafort, L.; Jolibois, F.; Olivucci, M.; Robb, M. A. *J. Am. Chem. Soc.* **2001**, *123*, 722.

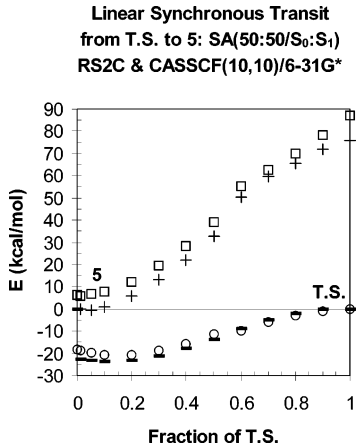

Figure 14. A view of the excited state along an LST, where TS = transition structure. For CASSCF, open circles are S_0 and open squares are S_1. For RS2C, dashes are S_0 and pluses are S_1.

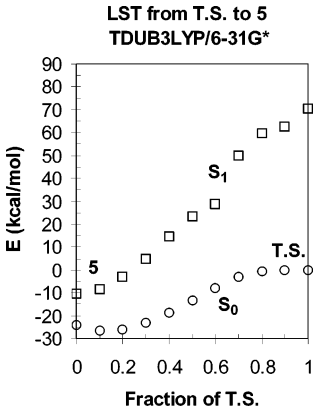

Figure 15. B3LYP view of the excited state along an LST, where TS = transition structure.

example, bioluminescence in the firefly[55] and chemiluminescence in 1,2-dioxetane decomposition.[56,57] More recently, we have suggested that the excited zwitterionic state of α,3-didehydrotoluene (**5**) may also be generated thermally by ring-opening of a carbene.[13]

Access to the S_1 surface from the cyclization transition structure was explored by way of a linear synchronous transit (LST), that is, the linearly interpolated path between the transition structure and zwitterion stationary points. SA(50:50/S_0:S_1)CAS(10,10) calculations performed along the LST between CAS(10,10)-optimized geometries revealed that the closest approach of S_1 and S_0 surfaces occurred near the geometry of the zwitterion (Figure 14). To refine this picture, SA(50:50/S_0:S_1)RS2C(10,10) energy corrections were performed (Figure 14). These revealed the zwitterion to be virtually isoenergetic with the transition structure. For the sake of comparison, an LST from the B3LYP transition structure to the RB3LYP zwitterion was constructed and TDUB3LYP was used to estimate the excited-state energies (Figure 15). This method gave a result qualitatively similar to the CAS results.[42]

In addition to the LST study, searches for avoided crossings or conical intersections close to the transition structure and zwitterion were carried out with SA(50:50/S_0:S_1)CAS(10,10) calculations. Four different geometries were used for four S_0/S_1 intersection searches. The input geometries were the CAS(10,10) transition structure, the CAS(10,10) zwitterion, a geometry from partway along the RB3LYP IRC, and the spurious RB3LYP cyclic allene geometry. In this same order, four different conical intersections (**11**, **12**, **13**, **14**) were found and were 27.4, 16.5, 37.2, and 15.1 kcal/mol above the S_0 state of the SA(50:50/S_0:S_1)CAS(10,10)//CAS(10,10) transition structure. Conical intersections **11** and **13** were not considered further because the other two were lower in energy. A RS2C correction, SA(50:50/S_0:S_1)RS2C(10,10), lowered the energies of **12** and **14** relative to the S_0 state of the SA(50:50/S_0:S_1)RS2C(10,10)//CAS(10,10) transition structure. For **12**, S_0 was 5.5 kcal/mol and S_1 was 8.8 kcal/mol, while for **14**, S_0 was 3.9 kcal/mol and S_1 was 6.2 kcal/mol. Because an intersection search at the RS2C level is currently intractable for a system of this size, the average of S_0 and S_1 was taken as an estimated value for the RS2C-corrected conical intersections[58] where **12** is 7.2 kcal/mol and **14** is 5.1 kcal/mol. These results support mechanisms **F** and **G** in that surface crossings, conical intersections **12** and **14** in this case, were found on the PE surface close to **5**, and their energies are accessible when one takes into account solvent effects (vide infra).

For the calculations to be in firm support of mechanisms **F** and **G**, some selective solvent stabilization of the zwitterion and any surface crossing (conical intersection) providing access to it must be invoked. However, predicting solvation effects on the S_1 surface and the conical intersections is not straightforward. Currently, it is not feasible to search for an intersection while simulating solvent effects, but because the lowest energy conical intersections are closest to the zwitterion,[59] it is assumed that as solvation decreases the energy of the zwitterion relative to the biradical, it will also decrease the energy of a conical intersection relative to the biradical. Therefore, the estimated solvation energy from Onsager model calculations[7] and polarized continuum model calculations for the zwitterion,[60] which are similar (~6 kcal/mol), could account for the 5 kcal/mol of solvation energy that is minimally required for the lowest energy conical intersection to be accessible.[61] Both plausible mechanisms in Figure 13 employ the zwitterion and invoke a nonadiabatic transition; the above results support the possibility of such a surface crossing.

(55) (a) White, E. H.; Roswell, D. F. *Photochem. Photobiol.* **1991**, *53*, 131. (b) Branchini et al. *J. Am. Chem. Soc.* **2002**, *124*, 2112 and references therein.
(56) Adam, W.; Heil, M.; Mosandl, T.; Saha-Möller, C. R. In *Organic Peroxides*; Ando, W., Ed.; John Wiley & Sons: Chichester, U.K., 1992; pp 221−254.
(57) (a) Tanaka, C.; Tanaka, J. *J. Phys. Chem. A* **2000**, *104*, 2078. (b) Wilsey, S.; Bernardi, F.; Olivucci, M.; Robb, M. A.; Murphy, S.; Adam, A. *J. Phys. Chem. A* **1999**, *103*, 1669.
(58) Pages, C. S.; Olivucci, M. *J. Comput. Chem.* **2003**, *24*, 289. Such an approximation was deemed acceptable based upon the results of Page and Olivucci. For five low lying S_0/S_1 conical intersections of small systems, they found that CAS and CASPT2 optimized structures were similar, and the difference in CASPT2 energies between the CAS- and CASPT2-optimized structures had an average difference of 2.1 kcal/mol.
(59) When generating linear-synchronous transits (LSTs), as in Figures 14 and 15, the *x*-axis is the fraction of one geometry with respect to both contributions and spans 0 to 1. Note that this coordinate serves its purpose if only two points are being compared. However, to compare three points and to have a qualitative view of the proximity of one point with respect to the other two, a different coordinate is necessary. In the present case, the approach was to use the components of a Z-matrix and take the sum of the squares of the differences (SSD) of these components between pairs of structures. The SSD will be small for structures that are similar and large for structures that are different. The SSD for a given pair of structures was used as the total "distance" between the two structures, although the units are mixed and have no physical meaning. For **12** and the TS, the SSD is 2.9, whereas for **12** and **5**, the SSD is 0.1. For **14** and the TS, the SSD is 3.4, whereas for **14** and **5**, the SSD is 0.6.

Conclusions

In an attempt to elucidate the source of benzylmethyl ether, this report rules out the methanol-assisted cyclization and presents evidence in support of the zwitterionic representation of α,3-didehydrotoluene (**5**) as the responsible intermediate. The implication for the reaction of nona-5,7,8-trien-3-yn-1-ol in methanol (Figure 8) is that the tethered alcohol traps the zwitterion and can go on to generate the observed products. In addition, enyneallene must directly form the zwitterion and exhibit a post-rate-determining bifurcation (Figure 12) in order to explain the experimental results of Hughes and Carpenter as well as Myers et al. Consequently, a post-transition state nonadiabatic transition from the ground-state singlet to an excited-state singlet is invoked, and this report presents theoretical results in support of this latter assertion. Few thermally induced organic reactions are known to exhibit such nonadiabatic behavior, which makes the present case intriguing.

Acknowledgment. We thank Professor W. T. Borden and co-workers David Hrovat and Christine Isborn for sharing their results, suggesting the dibenzoyl peroxide experiment, and for conducting some calculations on OH and CH hydrogen atom abstractions from methanol. We thank Stefan Debbert, Steve Kroner, and Aviva Litovitz for reviewing the manuscript. M.E.C. thanks Jeremiah Nummela and Antonio Ramirez for helpful discussions. Acknowledgment is made to the donors of The American Chemical Society Petroleum Research Fund for partial support of this research through Grant 40915-AC4.

Supporting Information Available: Cartesian coordinates, absolute energies, frequencies, and details for Figures 9, 10, 14, and 15. ^{13}C NMR spectrum of nona-5,7,8-3-yn-1-ol. This material is available free of charge via the Internet at http://pubs.acs.org.

JA0445443

(60) The zwitterion (constrained to be C_S) complexed with two water molecules was stabilized by 11.6 kcal/mol (ΔE_{elec}) relative to the triplet biradical complexed with two water molecules at the MP2/6-31+G** level of theory. This number increased by 5 kcal/mol to 17 kcal/mol when the complexes were reoptimized while including the solvent effect for methanol using the PCM. At the B3LYP/6-31G* level of theory, the zwitterion complexed with two water molecules was stabilized by 12.6 kcal/mol. These complexes were reoptimized while employing the Onsager model for methanol, and single-point PCM calculations on these complexes increased the stabilization energy by 7.5 kcal/mol to 20 kcal/mol. The solvent effect predicted by PCM for methanol is on the order of magnitude of 6 kcal/mol, which is similar to what Hughes and Carpenter observed for the uncomplexed zwitterion and biradical with the Onsager model.

(61) The 5 kcal/mol estimate was based on the RS2C-corrected energies for **14**.